Preprints of the 19th World Congress
The International Federation of Automatic Control
Cape Town, South Africa. August 24-29, 2014

Modeling Framework for investigating the Influence of Amino Acids on the Planktonic-Biofilm Transition of *Pseudomonas aeruginosa*

Zhaobin Xu, [1] Xin Fang, [2] Thomas K. Wood, [3] Zuyi (Jacky) Huang[1, 4, 5*]

1. Department of Chemical Engineering, Villanova University, Villanova, PA
2. The Henry M. Jackson Foundation for the Advancement of Military Medicine, Bethesda, MD
3. Departments of Chemical Engineering, Pennsylvania State University, University Park, PA
4. The Center for Nonlinear Dynamics & Control (CENDAC), Villanova University, Villanova, PA
5. Center for the Advancement of Sustainability in Engineering (VCASE), Villanova University, Villanova, PA

Abstract: The planktonic-biofilm transition is reported to facilitate the survival of disease-causing pathogens in a hostile environment, as the ability of pathogens to resist antibiotic treatment is 10 to 1000 times higher in a biofilm than in the planktonic mode. The availability of nutrient components such as amino acids in the surrounding environment plays an important role in the initiation of the biofilm formation. This work proposes a metabolic modeling framework to study the influence of availability of amino acids on the biofilm formation capability of *Pseudomonas aeruginosa*, one of the major pathogens causing nosocomial infections. Specifically, the genes that are up-regulated during the biofilm initiation were used to determine the metabolic reactions that are positively associated with *P. aeruginosa* biofilm formation. A criterion was then defined from the change of fluxes of these biofilm-associated reactions and the biomass growth rates to quantify the chance of biofilm formation upon the change of amino acid uptake rates. It was found that adding one of the following eleven amino acids, including Arg, Tyr, Phe, His, Iso, Orn, Pro, Glu, Leu, Val, and Asp, into the minimal medium may trigger *P. aeruginosa* biofilm formation. These results are perfectly consistent with the existing experimental data. The developed modeling framework was further used as an *in silico* platform to investigate the impact of the availability of two amino acids on the biofilm formation. It was found that the availability of additional amino acids can enhance biofilm formation and that there may be synergistic mechanisms for multiple amino acids to promote the biofilm formation.

1. INTRODUCTION

The biofilm is frequently involved in human infections. For example, biofilms are found on the surface of implanted cardiac devices in patients with heart-valve infection [1]. In addition, the antibiotic resistance capability of pathogens is enhanced significantly upon the formation of biofilms [2]. Investigation of the factors that influence the planktonic-biofilm transition is thus important for combating biofilm-associated pathogens. There are several modeling attempts for investigating the interactions of intracellular components such as genes, enzymes, and metabolites and thus identifying target genes to prevent the biofilm formation of *P. aeruginosa* [3, 4]. While microbial biofilm formation depends on both intracellular and extracellular factors, the impact from the extracellular factors that are characterized by the availability of environmental nutrients has not been systematically investigated. The availability of environmental nutrients has been proved to influence microbial biofilm formation [5]. Among those various nutrient components, amino acids, which supplement bacteria with nitrogen source, plays an especially important role in the biofilm formation. For example, certain strains of *Escherichia coli* K-12 and *Vibrio cholerae* cannot form biofilms in the minimal medium unless the medium is supplemented with amino acids [6]. In our previous approach, the genes that are up-regulated during the planktonic to biofilm transition of *P. aeruginosa* [7] were used to identify reactions that are positively related to the biofilm formation, and the change of fluxes of these reactions were then used to cluster genes according to the similarity of their mutants' ability to form a biofilm [4]. In this work, we further extended our previous work and proposed the first systematic approach to quantify the biofilm formation capability of *P. aeruginosa* upon different amino acid availabilities.

2. METHODS

2.1. Flux balance analysis

The flux balance analysis (FBA) is one of the most commonly used approaches to quantifying microbial growth for specific nutrient conditions. The metabolic network developed by Oberhardt et al., 2008 [8] is used in this work. It consists of 1056 metabolic genes, 1030 enzymes, and 883 metabolic reactions. Figure 1A lists a portion of metabolic reactions from the model, which is mathematically represented by the stoichiometric matrix **S** in Figure 1B. The nutrient condition is specified by the lower and upper bounds (i.e., lb_i and ub_i in Figure 1B) of the exchange reactions for nutrient components. Large upper bounds are assigned for

those nutrient components that are abundant in the surrounding environment and *vice versa*. It is assumed in FBA that bacteria try to grow as fast as possible from the available nutrients. Therefore, the biomass growth rate μ_{biomass} is maximized upon the constraints imposed by the mass balance and the lower/upper bounds of fluxes. This turns to a linear optimization problem where the maximal μ_{biomass} is determined from the solution space (Figure 1C). The COBRA toolbox developed by Dr. Palsson's group at UCSD is used in this work to perform the flux balance analysis [9].

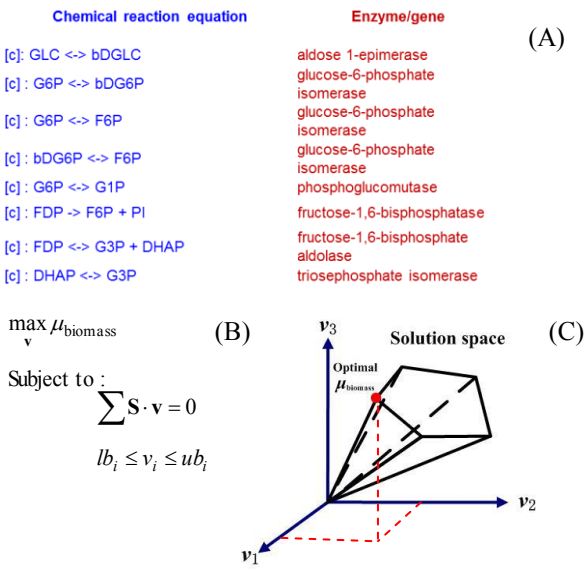

Figure 1, Schematic representation of FBA approach: (A) A small fraction of the metabolic reactions taken from the metabolic model, (B) the mathematical representation of the metabolic reaction networks where **S** is the stoichiometric matrix, μ_{biomass} is the biomass growth rate, **v** is the flux vector, lb_i and ub_i are the lower and upper bounds of flux v_i, (C) the optimal growth rate μ_{biomass} determined from the solution space via FBA.

2.2. An illustration example of the proposed approach

Figure 2 shows an illustrative example to describe our approach to quantifying the biofilm formation ability of *P. aeruginosa* for a specific nutrient condition. The change of the amino acid availability can be mimicked by changing the maximum uptake rate of amino acids in FBA. For example, a zero maximum uptake rate is assigned to arginine for the minimal medium without arginine (referred as reference nutrient condition), and a maximum 10 mmol $gDW^{-1}h^{-1}$ uptake rate is used to mimic the adding of arginine into the minimal medium (referred to as changed nutrient condition). This maximum arginine uptake rate is suggested by Oberhardt et al., 2008 [8]. FBA is then performed upon the metabolic model and the uptake constraints for both reference and changed nutrient conditions (Figure 2A). Biofilm-associated reactions are determined by overlaying the genes up-regulated during the planktonic-biofilm transition onto the metabolic network. The fluxes of these reactions, referred to as biofilm-associated reactions in Figure 2, are sampled for both reference and changed nutrient conditions (e.g., without and with arginine in the medium) (Figure 2B). The change of flux distribution of each biofilm-associated reaction upon the change of a single amino acid is quantified, based upon which the flux change curve for all biofilm-associated reactions is obtained (Figure 2C). Finally, this flux change curve and the biomass growth are used to determine the trend for planktonic *P. aeruginosa* to form biofilms upon the change of the availability of the amino acid (e.g., adding arginine into the minimal medium). Different from our previous approach in which the similarity among flux change curves for single gene-knockout mutants is used to cluster genes into different groups for identifying gene targets to treat *P. aeruginosa*, a new criterion named as biofilm formation capability is determined from the flux change curve in this work (see it in the Section 2.3) to quantify the trend of the planktonic *P. aeruginosa* to form biofilms. The biofilm formation capability is actually defined as the product of the ratio of growth rate and the ratio of the fluxes through biofilm-associated reactions for the changed availability of the target amino acid (e.g., the minimal medium with the addition of arginine) over the ones for the reference condition (e.g., the minimal medium). Since *P. aeruginosa* is in the planktonic growth mode in the reference nutrient condition, the change of fluxes over biofilm-associated reactions can indicate the trend of the pathogen to form a biofilm upon the changed availability of the target amino acid. The flux change via the biofilm associated reactions thus quantifies the biofilm formation of individual *P. aeruginosa*, while the product of flux change with the growth rate represents the biofilm formation capability of a population of planktonic *P. aeruginosa*. The proposed approach can be easily applied to study the impact of the change of the availability of multiple amino acids on the biofilm formation, as the up-take rates of multiple amino acids can be changed simultaneously in FBA.

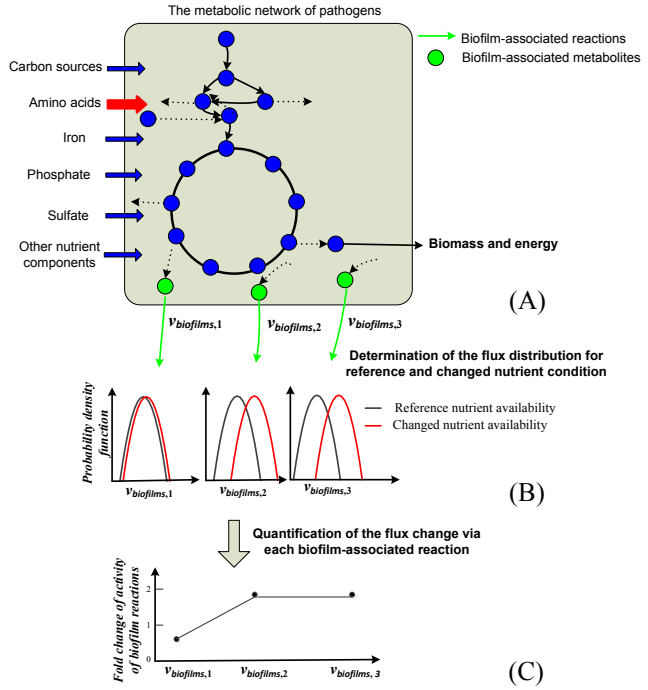

Figure 2, an illustrative example to show the proposed approach for quantifying the biofilm formation of *P. aeruginosa* for different availabilities of amino acids: (A)

The availability of the amino acid is represented by its maximum uptake rate in FBA; (B) Flux distribution of those biofilm-associated reactions is determined for both reference and changed amino acid availability; (C) the flux-change curve over all biofilm-associated reactions is quantified upon the change of the amino acid availability. It is then multiplied with the change of growth rate to quantify the microbial biofilm formation.

2.3. The approach to quantify the capability of planktonic *P. aeruginosa* to form biofilms for different availabilities of amino acids

The similarity in the shape and magnitude of the flux change curve (Figure 1C) were used by our previous approach [4] to cluster single mutants into different groups to identify the gene targets for eliminating planktonic *P. aeruginosa* before it forms a biofilm. However, no approach has been proposed to directly quantify biofilm formation capability of planktonic *P. aeruginosa* from the flux change curve, in which the flux changes of different biofilm-associated reactions are quite different. To address this, we define a new criterion from the flux change curve to quantify the capability of planktonic *P. aeruginosa* to form a biofilm in this section. In addition, we formulate an approach to solve a problem that has not been systemically investigated, that is, how to quantify the influence of the availability of amino acids on the *P. aeruginosa* biofilm formation. Our approach consists of the following steps.

Step 1: define the reference and changed availability of amino acids in the medium

The minimal medium is used as the reference nutrient condition for studying the influence from amino acids on *P. aeruginosa* biofilm formation. Only one amino acid is added at a time to the minimal medium to mimic a changed amino acid availability. These changed nutrient conditions are studied in this work as experimental data are existing for these conditions to validate our approach.

Step 2: The fluxes of each biofilm-associated reaction are sampled for both the reference and changed nutrient conditions via the artificial-center-hit-and-run (ACHR) sampling approach from the COBRA toolbox [9].

Fluxes are sampled here, as the optimal flux solution **v** for FBA is typically not unique, that is, multiple values of **v** can return the same optimal growth rate μ_{biomass} [9]. The sampled fluxes for each biofilm-associated reaction are analyzed to quantify the mean value, and the probability density function of fluxes in the solution space, which are represented by $\mu_{v_n}^{\text{reference}}$ and $f_{v_n}^{\text{reference}}$ for the reference nutrient condition and $\mu_{v_n}^{\text{changed}}$ and $f_{v_n}^{\text{changed}}$ for the changed nutrient condition (Figure 3). n is the index of a biofilm-associated reaction.

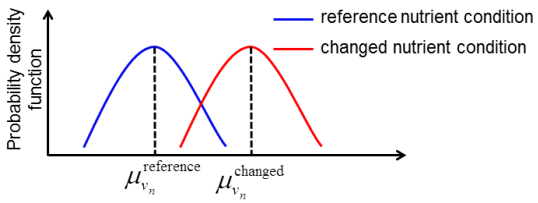

Figure 3, the distributions of fluxes via the nth biofilm reaction for both the reference and changed nutrient conditions. Both the probability density function and the mean value are determined for each distribution.

The change in the flux distribution of each biofilm-associated reaction upon the change of amino acid availability is quantified by $\mu_{v_n}^{\text{reference}}$ and $\mu_{v_n}^{\text{changed}}$ via Equation (1)

$$Flux\_Var_{v_n}^{\text{a-acid}\,m} = \frac{\mu_{v_n}^{\text{changed}}}{\mu_{v_n}^{\text{reference}}} \times KS(f_{v_n}^{\text{changed}}, f_{v_n}^{\text{reference}}) \qquad (1)$$

where $Flux\_Var_{v_n}^{\text{a-acid}\,m}$ quantifies relative flux change when the availability of amino acid m is switched from the reference to the changed condition, KS(·) is a two-sample Kolmogorov-Smirnov test in which the test result is equal to one/zero if the distribution $f_{v_n}^{\text{changed}}$ is statistically/not different from $f_{v_n}^{\text{reference}}$.

Equation (1) is used to quantify the flux change curve through all the biofilm-associated reactions, which can be represented by the vector **Vector_flux_var** shown in Equation (2).

$$\mathbf{Vector\_flux\_var} = [Flux\_Var_{v_1}^{\text{a-acid}\,m}\ Flux\_Var_{v_2}^{\text{a-acid}\,m} \cdots Flux\_Var_{v_n}^{\text{a-acid}\,m}] \qquad (2)$$

Step 3: Equation (3) is used to quantify the flux change via the biofilm-associated reactions upon the change of amino acid m.

$$r_{\text{flux}}^{\text{a-acid}\,m} = \sqrt{\frac{\sum_{i=1}^{n}(Flux\_Var_{v_i}^{\text{a-acid}\,m})^2 \times sign(Flux\_Var_{v_i}^{\text{a-acid}\,m})}{n}} \qquad (3)$$

where the sign (·) function is equal to one if the flux through the biofilm-associated reaction v_i doesn't change its direction upon the change of the availability of amino acid m. The rationale behind this is that reaction v_i is positively associated with the biofilm formation and a changed flux direction means the trend to form biofilms reverses.

Step 4: Equation (4) is used to quantify the biofilm formation capability upon the change of amino acid m.

$$C_{\text{biofilm}}^{\text{a-acid}\,m} = r_{\text{flux}}^{\text{a-acid}\,m} \times r_{\text{growth}}^{\text{a-acid}\,m} \qquad (4)$$

where $r_{\text{growth}}^{\text{a-acid}\,m}$ is the ratio of the growth rate for the medium with and without the added amino acid. $C_{\text{biofilm}}^{\text{a-acid}\,m}$ indicates the planktonic-biofilm transition capability of *P. aeruginosa* upon the change of the availability of amino acid m. A value of $C_{\text{biofilm}}^{\text{a-acid}\,m}$ that is significantly larger than one means that the

planktonic *P. aeruginosa* may switch to the biofilm growth mode once the availability of amino acid *m* is changed from the reference to the changed condition.

3. SIMULATION RESULTS AND DISCUSSION

3.1. Determination of 39 metabolic reactions positively correlated to biofilm formation

39 metabolic reactions were identified positively correlated to the biofilm formation via the approach shown in our previous work [4]. As shown in Figure 4, these biofilm-associated reactions are mainly involved in amino acid metabolism, ion metabolism, acetate metabolism, pyrimidine metabolism, TCA cycle, oxidative phosphorylation, and co-enzyme B12 metabolism. The 39 biofilm reactions are listed in the appendix.

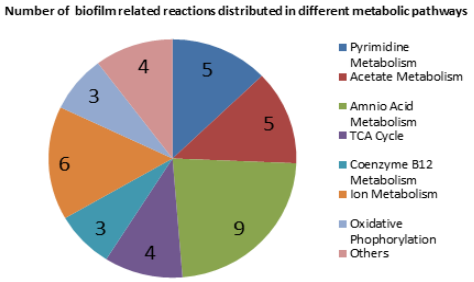

Figure 4, the distribution of the 39 reactions that positively indicate the planktonic-biofilm transition of *P. aeruginosa* in the metabolic network

3.2. Influence of the availability of single amino acid on *P. aeruginosa* biofilm initiation

Based upon the change of fluxes of the 39 biofilm reactions determined in the previous section, the trend for planktonic *P. aeruginosa* to form biofilm upon single amino acid addition into the minimal medium was quantified in this section. The minimal medium was used as the reference nutrient condition in which no amino acid is supplied. Only one amino acid was added into the minimal medium at a time, which represented a changed nutrient condition. The capability of planktonic *P. aeruginosa* to form a biofilm for each added amino acid was determined and shown in Figure 5. The experimental data from Bernier et al., 2011 [10] that quantified the biofilm formation of *P. aeruginosa* for the same conditions are also shown in this figure. It can be seen from Figure 5 that the top *in-silico* ranked amino acids also lead to enhanced biofilm formation in experiment. This indicates an excellent match between the modeling results and the existing experimental data. In addition, those amino acids with low biofilm formation ability in Figure 5 are predicted by our approach to not significantly induce the planktonic-biofilm transition of *P. aeruginosa*, as fluxes via those biofilm associated reactions don't change that much upon the change of the amino acid availability. This is consistent with the experimental data, which also indicate that the supplement of each of these amino acids in the minimal medium cannot significantly induce *P. aeruginosa* biofilm formation. The detailed mechanisms of amino acids' promotion effects on biofilm formation are still under investigation in the biofilm community, although some cues have been discovered for limited amount of amino acids. For example, enhanced availability of arginine is able to promote the *P. aeruginosa* biofilm formation [10], as additional arginine may up-regulate the intracellular levels of c-di-GMP, which in turn stimulates biofilm formation. Our approach provides a modeling framework to systematically reveal the underlying mechanisms of nutrient components like amino acids to promote the biofilm formation, as the change of fluxes of all metabolic reactions can be determined and analyzed. Only the flux change of the 39 biofilm-associated reactions is shown and analyzed in this work due to the space limitation. Another advantage of our approach is that we can incorporate the change of environmental amino acids by changing the uptake rates of the exchange reactions of amino acids without including the complicated signaling pathways that are implemented by the cells to sense the change of amino acids in the surrounding environment.

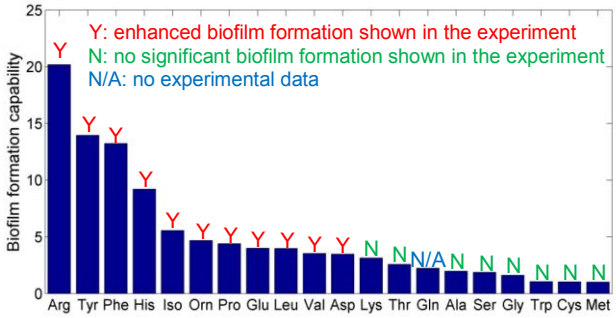

Figure 5, the biofilm formation capability of planktonic *P. aeruginosa* upon adding each of the 20 amino acids into the minimal medium. The minimal medium is used as the reference condition, while adding each of the 20 amino acids is referred to as the changed nutrient condition.

3.3. Influence of the availability of arginine on *P. aeruginosa* biofilm formation

In the previous section, a maximum uptake rate of 10 mmol $gDW^{-1}h^{-1}$, which is suggested by Oberhardt et al., 2008 [8], was set for each amino acid. One interesting problem to investigate here is how the biofilm formation and growth rate change with different availabilities for a specific amino acid (i.e., different maximum uptake rates). We thus studied *P. aeruginosa* biofilm formation for various maximum uptake rates of arginine, which mimics different availabilities of arginine in the medium. Arginine is chosen as the example amino acid for investigation here is because arginine displays the most significant influence on *P. aeruginosa* biofilm enhancement (as shown in Figure 5). As shown in Figure 6, the growth rate of *P. aeruginosa* increases almost linearly with the increase of arginine maximum uptake rate, which indicates the important role of arginine in promoting the growth of *P. aeruginosa*. Figure 6 also show that the biofilm formation also increases with increasing uptake rates of arginine. This further confirms the availability of arginine for the formation of *P. aeruginosa* biofilm.

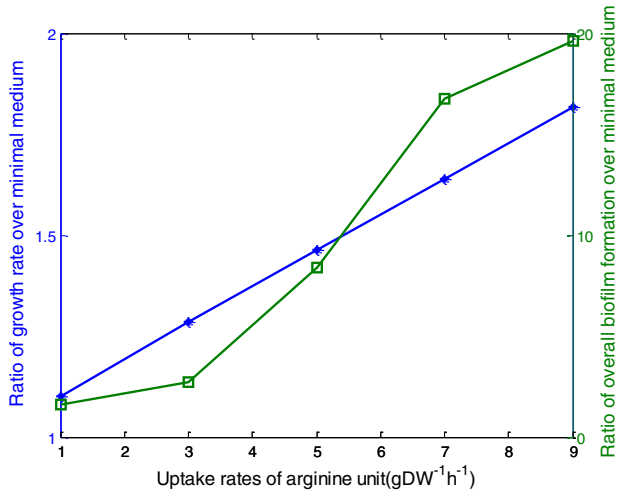

Figure 6, the biofilm formation capability and growth rates of planktonic *P. aeruginosa* upon different availabilities of arginine in the medium.

3.4. Influence of two added amino acids in the medium on *P. aeruginosa* biofilm formation

The results shown so far are focused on the influence of the availability of a single amino acid on *P. aeruginosa* biofilm formation. Our approach was then extended to investigate the influence of multiple nutrient components such as amino acids on the planktonic-biofilm transition of *P. aeruginosa*. As an example, the influence of adding each two amino acids into the minimal medium on the biofilm formation was evaluated by setting the maximum uptake rates of the two amino acids to the recommended value of 10 mmol $gDW^{-1}h^{-1}$ in the flux balance analysis. There are 190 combinations of two amino acids in the simulation. Only the 10 combinations of amino acids that enhance *P. aeruginosa* biofilm formation the most is listed in Table 1. As shown in this table, arginine is involved in 9 of the 10 double amino acid combinations. This can be explained by the importance of arginine on *P. aeruginosa* biofilm formation. However, the ranking sequence shown in Table 1 does not totally follow the linear combination of the influence of each individual amino acid that is shown in Figure 5. For instance, while adding lysine itself promotes much less biofilm than that for adding tyrosine (as shown in Figure 5), the combination of arginine and lysine induce a stronger biofilm formation than the combination of arginine and tyrosine. Another example is given by the combination of alanine and ornine, each of which induce less biofilm than arginine or tyrosine, can induce more biofilm formation than the combination of arginine or tyrosine. This implies that there may be synergistic mechanisms for multiple amino acids to promote the biofilm formation. This is an interesting topic for further investigation. In addition, adding another amino acid to the medium generally enhance the biofilm formation. As shown in Table 1, adding another amino acid to the medium with arginine induces more biofilm formation when comparing $C_{\text{biofilm}}^{\text{a-acid m}}$ shown in Table 1 to that in Figure 5.

Table 1. The growth rate and biofilm formation capability for adding two amino acids into the minimal medium

Amino acids	$r_{\text{growth}}^{\text{a-acid m}}$	$r_{\text{flux}}^{\text{a-acid m}}$	$C_{\text{biofilm}}^{\text{a-acid m}}$
Arg and Lys	1.9038	15.1334	28.8106
Ala and Orn	1.9038	15.1334	28.8106
Arg and Thr	1.9038	13.9367	26.5326
Arg and Tyr	1.9037	13.3956	25.5016
Arg and Trp	1.9038	12.7526	24.2782
Arg and Iso	1.9039	12.3898	23.589
Arg and Met	1.9037	12.3888	23.585
Arg and Orn	1.9038	11.186	21.2959
Arg and Glu	1.9039	11.0404	21.0203
Arg and Val	1.9038	10.8905	20.7335

4. CONCLUSIONS

The biofilm is often associated with human diseases, as it can protect pathogens from the treatment of antibiotics. This work presented the first systems biology approach to quantify the planktonic-biofilm transition of *P. aeruginosa* upon the change of nutrient conditions that are characterized by the availability of nutrient components including twenty amino acids. The results for adding one amino acid at a time into the minimal medium match very well with the existing experimental data. It is found that adding each of the eleven amino acids that include Arg, Tyr, Phe, His, Iso, Orn, Pro, Glu, Leu, Val, and Asp in the minimal medium, promotes the planktonic-biofilm transition of *P. aeruginosa*. The biofilm formation ability of *P. aeruginosa* upon different availabilities of arginine was also evaluated. An increasing availability of arginine is found to promote both the microbial growth and the biofilm formation. This further confirms the importance of arginine for *P. aeruginosa* biofilm formation. The developed approach was finally extended to evaluate the influence of adding two amino acids into the minimal medium on biofilm formation of *P. aeruginosa*. It is found that adding multiple amino acids can enhance biofilm formation when compared to the addition of a single amino acid. In addition, there may be synergistic mechanisms for multiple amino acids to promote the biofilm formation.

Although this work mainly studied P. aeruginosa biofilm formation upon the change of nutrient conditions, our approach can be applied to any other microorganism if a metabolic model is available for it and the biofilm-associated reactions can be determined accordingly. In addition, the developed approach can be also applied to study the influence of other nutrient components such as carbon sources and ion on the initial transition of planktonic *P. aeruginosa* to the biofilm growth mode. This study is valuable in guiding the prevention of biofilm formation of *P. aeruginosa* through controlling the nutrient supply.

REFERENCES

1. Douglas, L.J., *Candida biofilms and their role in infection.* Trends Microbiol, 2003. **11**(1): p. 30-6.
2. Stoodley, P., et al., *Biofilms as complex differentiated communities.* Annu Rev Microbiol, 2002. **56**: p. 187-209.
3. Sigurdsson, G., et al., *A systems biology approach to drug targets in Pseudomonas aeruginosa biofilm.* PLoS One, 2012. **7**(4): p. e34337.
4. Xu, Z., et al., *A systems-level approach for investigating Pseudomonas aeruginosa biofilm formation.* PLoS One, 2013. **8**(2): p. e57050.
5. Kristich, C.J., et al., *Esp-independent biofilm formation by Enterococcus faecalis.* J Bacteriol, 2004. **186**(1): p. 154-63.
6. Watnick, P.I., K.J. Fullner, and R. Kolter, *A role for the mannose-sensitive hemagglutinin in biofilm formation by Vibrio cholerae El Tor.* J Bacteriol, 1999. **181**(11): p. 3606-9.
7. Musken, M., et al., *Genetic determinants of Pseudomonas aeruginosa biofilm establishment.* Microbiology, 2010. **156**(Pt 2): p. 431-41.
8. Oberhardt, M.A., et al., *Genome-scale metabolic network analysis of the opportunistic pathogen Pseudomonas aeruginosa PAO1.* J Bacteriol, 2008. **190**(8): p. 2790-803.
9. Schellenberger, J., et al., *Quantitative prediction of cellular metabolism with constraint-based models: the COBRA Toolbox v2.0.* Nat Protoc, 2011. **6**(9): p. 1290-307.
10. Bernier, S.P., et al., *Modulation of Pseudomonas aeruginosa surface-associated group behaviors by individual amino acids through c-di-GMP signaling.* Res Microbiol, 2011. **162**(7): p. 680-8.

APPENDIX

Supplemental Table 1. The 39 biofilm-associated reactions [4]

Reactions	Genes
Rxn#1: dGTP + H_2O → Deoxyguanosine + Inorganic triphosphate	PA1124 (*dgt*)
Rxn#2: GTP + H_2O → Guanosine + Inorganic triphosphate	PA1124 (*dgt*)
Rxn#3: H+ + Malonate → Acetate + CO_2	PA0208 (*mdcA*)
Rxn#4: Coenzyme A + 3-Oxoadipyl-CoA → Acetyl-CoA + Succinyl-CoA	PA0228 (*pcaF*)
Rxn#5: 4-Aminobutanoate + 2-Oxoglutarate → L-Glutamate + Succinic semialdehyde	PA0266 (*gabT*)
Rxn#6: 2 S-Adenosyl-L-methionine + Uroporphyrinogen III → 2 S-Adenosyl-L-homocysteine + H+ + Dihydrosirohydrochlorin	PA0510 (*nirE*)
Rxn#7: Ferrocytochrome c + 2 H+ + Nitrite → Ferricytochrome c + H_2O + Nitric oxide	PA0511 (*nirJ*)
Rxn#8: Fumarate + H_2O ↔ L-Malate	PA0854 (*fumC2*)
Rxn#9: $cobalt_2$[e] → $cobalt_2$[c]	PA0913 (*mgtE*)
Rxn#10: mg2[e] → mg2[c]	PA0913 (*mgtE*)
Rxn#11: 1-Aminopropan-2-ol + Adenosyl-cobyric acid ↔ Adenosyl cobinamide + H_2O	PA1275 (*cobD*)
Rxn#12: L-Threonine → 2-Oxobutanoate + Ammonium	PA1326 (*ilvA2*)
Rxn#13: 4-Maleylacetoacetate → 4-Fumarylacetoacetate	PA2007 (*maiA*)
Rxn#14: Benzoate + 2 H+ + Nicotinamide adenine dinucleotide - reduced + O_2 → Cis-1,2-dihydroxycyclohexa-3,5-diene-1-carboxylate + Nicotinamide adenine dinucleotide	PA2518 (*xylX*)
Rxn#15: Isocitrate + Nicotinamide adenine dinucleotide phosphate ↔ 2-Oxoglutarate + CO_2 + Nicotinamide adenine dinucleotide phosphate - reduced	PA2623 (*icd*)
Rxn#16: 3 H+ + Nicotinamide adenine dinucleotide - reduced + Ubiquinone-8 → Nicotinamide adenine dinucleotide + Ubiquinol-8 + 2 H+	PA2642 (*nuoG*)
Rxn#17: ATP + H_2O + Phosphonate[e] → ADP + H+ + Phosphate + Phosphonate[c]	PA3383 (*phnD*)
Rxn#18: S-Adenosyl-L-methionine + Butyryl-[acyl-carrier protein] → 5-Methylthioadenosine + Acyl carrier protein + H+ + N-butyryl-L-homoserine lactone	PA3476 (*rhlI*)
Rxn#19: 2 Ferrocytochrome c + 4 H+ + 0.5 O_2 → 2 Ferricytochrome c + H_2O + 2 H+	PA4133 (*ccoN*)
Rxn#20: ATP + H_2O + Fe-enterobactin → ADP + Fe-enterobactin + H+ + Phosphate	PA4160 (*fepD*)
Rxn#21: Chorismate → Isochorismate	PA4231 (*pchA*)
Rxn#22: 2 Hydrogen peroxide → 2 H_2O + O_2	PA4236 (*katA*)
Rxn#23: Alpha-D-Ribose 5-phosphate + Uracil ↔ H_2O + Pseudouridine 5'-phosphate	PA4544 (*rluD*)
Rxn#24: 1.5 O_2 + Protoporphyrinogen IX → 3 H_2O + Protoporphyrin	PA4664 (*hemK*)
Rxn#25: Alpha-Oxo-benzeneacetic acid ↔ Benzaldehyde + CO_2	PA4901 (*mdlC*)
Rxn#26: Reduced glutathione + Methylglyoxal → (R)-S-Lactoylglutathione	PA5111 (*gloA3*)
Rxn#27: N(omega)-(L-Arginino)succinate ↔ L-Arginine + Fumarate	PA5263 (*argH*)
Rxn#28: ATP + H_2O + Phosphate[e] → ADP + H+ + 2 Phosphate[c]	PA5368 (*pstC*)
Rxn#29: Citrate[e] + H+[e] ↔ Citrate[c] + H+[c]	PA5476 (*citA*)
Rxn#30: 5,6-dihydrouracil + H_2O ↔ N-Carbamoyl-beta-alanine + H+	PA0441 (*dht*)
Rxn#31: Nicotinamide adenine dinucleotide + O-Phospho-4-hydroxy-L-threonine → 2-Amino-3-oxo-4-phosphonooxybutyrate + H+ + Nicotinamide adenine dinucleotide – reduced	PA0593 (*pdxA*)
Rxn#32: 2-Methyl-4-amino-5-hydroxymethylpyrimidine diphosphate + 4-Methyl-5-(2-phosphoethyl)-thiazole + H+ → Diphosphate + Thiamin monophosphate	PA3976 (*thiE*)
Rxn#33: ATP + Coenzyme A + Succinate ↔ ADP + Phosphate + Succinyl-CoA	PA1588 (*sucC*)
Rxn#34: L-Aspartate + ATP + L-Citrulline → AMP + N(omega)-(L-Arginino)succinate + H+ + Diphosphate	PA3525 (*argG*)
Rxn#35: Acetate + ATP + Coenzyme A → Acetyl-CoA + AMP + Diphosphate	PA4733 (*acsB*)
Rxn#36: 2 ATP + L-Glutamine + H_2O + Bicarbonate → 2 ADP + Carbamoyl phosphate + L-Glutamate + 2 H+ + Phosphate	PA4758 (*carA*)
Rxn#37: 2 H+ + H_2O + Urea → CO_2 + 2 Ammonium	PA4867 (*ureB*)
Rxn#38: H_2O + Urocanate → 4-Imidazolone-5-propanoate	PA5100 (*hutU*)
Rxn#39: ATP + Oxaloacetate → ADP + CO_2 + Phosphoenolpyruvate	PA5192 (*pckA*)